Computational Study of 16S rRNA of Microbe Cluster Implicated in Diarrhoeal: Phylogeny, Docking, and Dynamics

Harriet U. Ugboko
Covenant University, Ota, Ogun State, Nigeria. https://orcid.org/0000-0002-7000-8978
Toluwase Hezekiah Fatoki (hezekiahfatoki@gmail.com)
Federal University Oye-Ekiti, Ekiti State, Nigeria. https://orcid.org/0000-0003-3202-9855
Obinna C. Nwinyi
Covenant University, Ota, Ogun State, Nigeria.
Omodele Ibraheem
Federal University Oye-Ekiti, Ekiti State, Nigeria. https://orcid.org/0000-0003-1011-7061
Conrad A. Omonhinmin
Covenant University, Ota, Ogun State, Nigeria.
Jesupemi Mercy Fatoki
Federal University of Technology, Akure, Ondo State, Nigeria. https://orcid.org/0000-0002-7595-5229
Oluwafijimi Yomi Adetuyi
Federal University Oye-Ekiti, Ekiti State, Nigeria.

Research Article

Keywords: 16S rRNA, diarrhoea, 2D and 3D structure, antibiotics, molecular docking, drug-enzyme-RNA interactions

Posted Date: October 19th, 2021

DOI: https://doi.org/10.21203/rs.3.rs-984331/v1

Abstract

In this study, 16S rRNA of diarrhoea microbial cluster was investigated computationally. The phylogeny, two- and three-dimensional structures, molecular docking and dynamics simulations were carried out. The result showed that *Escherichia coli, Campylobacter jejuni, Campylobacter upsaliensis, Streptococcus lutetiensis* 033, *Streptococcus infantarius, Enterococcus ratti, Helicobacter sp.* 'feline isolate, *Helicobacter canadensis, Anaerobiospirillum* sp. B0101, *Anaerobiospirillum* sp. 3J102 as well as uncultured bacterium (*Prevotella*) and unidentified bacterium (*Lactobacillus*) were involved in diarrhoea infection. Optimal secondary structure alignment from ClustalO has a minimum free energy (MFE) of -764.31 kcal/mol while that Aligner has MFE of -592.43 kcal/mol. The free energies from molecular docking reveal possible efficacy in the order of doxycycline > metacycline > streptomycin > rolitetracycline > tetracycline > tigecycline. Out of 17 antibiotics used in this study, chlortetracycline and minocycline have high affinity for methyltransferase KsgA (PDB ID: 3TPZ), kanamycin has almost equal affinity for both enzymes, while the remaining 14 antibiotic compounds have high affinity for pseudouridine synthase RsuA (PDB ID: 1KSV). The modelled three-dimensional structure of 16S rRNA bind to 1KSV and 3TPZ with free energy of -367.52 kcal/mol and-371.55 kcal/mol respectively. Moreover, the active site nucleotide residues were found to have direct interaction with amino acid residues in the active site of the enzymes. This study provides insight on the mechanism of action of antibiotics that targeted 16S rRNA by inhibition of key enzymes that involve in protein synthesis.

Introduction

The human body serves as a host to billions of microorganisms (bacteria, viruses, fungi, and protozoa) with a large functional diversity that surpasses the human gene pool, which can bring health outcome through interplay (parasitic/pathogen or symbiotic/commensal) with human cells based on the level of exposure (Qin et al., 2010; Yang et al., 2016; Singh et al., 2017). The microbiome of children is not fully stable and varies inter-individually from the maternal microbial status, and subsequent exposure to different environmental conditions, dietary patterns, and antimicrobial drugs (Tamburini et al., 2016; Hill et al., 2017). A diverse and balanced gut microbiome provides benefits to the host by modulating several physiological processes such as biosynthesis and systemic bioavailability of nutrients, regulation of host intermediary metabolism, development of the immune system, and metabolism of bioactive compounds (Wu et al., 2015; Yang et al., 2016).

Diarrhoea, a gastrointestinal disease which has been consistently caused over one million childhood mortality per year worldwide (Ugboko et al., 2019). The occurrence of childhood mortality in developing countries due to diarrhoea disease is between 9%-34% (WHO, 2015). Diarrhoea is associated with an ecological imbalance of the intestinal microbiota which consists of hundreds of species. The underlying complexity as well as individual differences between patients can contributes to the difficulty faced in the efficacy of the current therapeutics.

Enterotoxigenic *Escherichia coli* (ETEC) remains a major cause of diarrhoea-associated mortality and morbidity of infants, young adults and adults in endemic areas (Lamberti et al., 2014). Bioinformatics and metagenomic studies of diarrhoea have reported the presence of *E. coli*, *C. jejuni, Clostridium difficile*, *Helicobacter pylori, Salmonella typhi, Shigella flexneri* and *Vibrio cholera* (Loman et al., 2013; Ugboko et al., 2019), while existing viruses can serve as causative agents of diarrhoea, such as noroviruses, rotaviruses, astroviruses, sapovirus, and enteric adenoviruses (Dycke et al., 2018). Chronic diarrhea is often a critical problem for patients infected with the human immunodeficiency virus (HIV), where it decreases response to antiretroviral therapy and quality of life in general (Oldfield, 2002).

Metagenomic study has shown that multiple mechanisms drive microbial succession after cholera, including bacterial dispersal properties, changing enteric oxygen and carbohydrate levels, and phage dynamics (David et al., 2015). Ribonucleic acid (RNA) sample has been used for transcriptional analysis of cell in microgravity and investigation of antibiotic resistance (Zhang et al., 2019). Sequencing of rRNA gene is a well-utilized method for nucleic acid-based detection and identification of microbes, their taxonomic assignment, phylogenetic analysis and the study of microbial diversity (Quast et al., 2013). The 16S rRNA is a generally accepted target for many of antibiotics but the actual mechanism of action has not been fully comprehended. In this study, the biology of 16S rRNA of diarrhoea microbe cluster was investigated computationally, to understand its pharmacological potentials.

Methods

In silico **preparation of 16S rRNA sequences**

The 16S rRNA of cluster of microbes involve in diarrhoea was obtained by searching “diarrhea” under publication and RefNR, in SILVA ribosomal RNA small subunit (SSU) gene database (https://www.arb-silva.de/search/; Quast et al., 2013). The sequences of reference genome of all the listed microbes were download in FASTA without gap format.

Phylogenetic analysis

Multiple sequence alignment (MSA) of the 16S rRNA sequences of diarrhea-related microbes that were found were carried out on Aligner server (www.arb-silva.de/aligner/) and ClustalO server respectively and phylogenetic tree was constructed. The phylogenetic tree was visualized on iTOL server (https://itol.embl.de/upload.cgi; Letunic and Bork, 2019).

Structural analysis

The MSA from Aligner and ClustalO of 16S rRNA sequences with pintail quality were used respectively to predict the consensus secondary structure (CSS) using RNAalifold (http://rna.tbi.univie.ac.at/cgi-bin/RNAWebSuite/RNAalifold.cgi; Bernhart et al., 2008) and saved as Vienna format. The structure sequence in Vienna format for ClustalO sample was edited to remove gaps and used as sequence of CSS for three-dimensional (3D) modeling during enzyme-RNA molecular docking.

Drug-enzyme molecular docking

Drugs indicated for 16S rRNA in the DrugBank (www.drugbank.ca/bio_entities/BE0004799) were used as ligands for molecular docking study against *E. coli* (strain K12) 16S rRNA pseudouridine synthase (PDB ID: 1KSV; Sivaraman et al., 2002) and 16S rRNA methyltransferase KsgA (PDB ID: 3TPZ; O'Farrell et al., 2012). The structures of the compounds were obtained from PubChem Compound database of NCBI in .sdf format and then converted to .pdb file using PyMol v2.0.7. The molecular docking studies were carried out according to the method of Ibraheem et al. (2019), where all water molecules and bounded compounds were removed from the crystal structure of the 1KSV using PyMol v2.0.7 while polar hydrogens were added and AutoDock Tools (ADT) v1.5.6 (Morris et al., 2009). Target protein and ligands were prepared for docking using ADT at default settings, and the output file was saved in pdbqt format. The grid parameter for 1KSV (chain A) were center grid box (points): 40.417 x 19.372 x -4.566; size (points): 126 x 106 x 96; and spacing (Å): 0.575, while grid parameter for 3TPZ (chain A) were: center grid box (points): 89.834 x 5.542 x 12.530; size (points): 126 x 84 x 74; and spacing (Å): 0.575. Molecular docking program AutoDock Vina v1.1.2 (Trott and Olson, 2010) was employed to perform the blind docking experiment. After docking, close interactions of binding of the target with the ligands were analyzed and visualized using ADT

Enzyme-RNA molecular docking

The HDOCK server (http://hdock.phys.hust.edu.cn/; Yan et al., 2017; Huang and Zou, 2014) was used for 3D modeling of sequence of CSS sequence obtained in previous step. The RNA structure was built using template-free method, and docked to the PDB structure of 1KSV and 3TPZ respectively, which were prepared in previous step. After docking, the best RNA-protein binding pose was obtained and visualized on the HDOCK server while binding RNA residues were identified using PyMol v2.0.7.

Ligand-Protein Dynamics Simulation

The molecular dynamics of the interaction of Doxycycline and Methacycline with methyltransferase KsgA (PDB ID: 3TPZ), were investigated respectively on LARMD server (http://chemyang.ccnu.edu.cn/ccb/server/LARMD/) at Int_mod for 1 ns in an explicit water model (Yang et al., 2019). LARMD provides an automatic protocol for conformational sampling and analysis. Root-mean-square deviation (RMSD), radius of gyration (Rg) and fraction of native contacts (Q), principal component analysis (PCA), and molecular mechanics Poisson–Boltzmann or Generalized Born surface area (MM-PB/GBSA), were evaluated.

Protein SWAXS Dynamics Simulation

Small- and wide-angle X-ray scattering (SWAXS) curves based on explicit-solvent all-atom molecular dynamics (MD) simulations were calculated on WAXSiS server (http://waxsis.uni-goettingen.de). The protein PDB IDs (1KSV and 3TPZ (chain A) respectively) were used to query the server with retention of existing ligands that bounded to the protein while others parameters were at default setting of the server.

SWAXS is used to detect global parameters of biomolecules, such as the radius of gyration, the multimeric state, or aggregation (Knight and Hub, 2015).

Results

This study (as shown in Table 1 and Figure 1), identifies the involvement of *E. coli, C. jejuni, Streptococcus lutetiensis 033, Streptococcus infantarius, Campylobacter upsaliensis, Enterococcus ratti, Helicobacter sp.* 'feline isolate, *Helicobacter canadensis, Anaerobiospirillum sp. B0101, Anaerobiospirillum sp. 3J102* as well as uncultured bacterium (*Prevotella*) and unidentified bacterium (*Lactobacillus*). Ribosome is the site of protein synthesis in the cell, which based on the genetic information in deoxyribonucleic acids (DNA) that transcribes to ribonucleic acids (RNA). This study identifies difference in the secondary (2D) structure of consensus 16S rRNA produced by RNAalifold from ClustalO server and Aligner server multiple sequence alignments (MSA) (Figure 2 and 3). The optimal secondary structure (SS) from ClustalO MSA has a minimum free energy (MFE) of -764.31 (-383.21 plus -381.10 from covariance contributions) kcal/mol, free energy of the thermodynamic ensemble is -785.70 kcal/mol and frequency of the MFE structure in the ensemble is 0.00%, while that Aligner MSA has a MFE of -592.43 (-299.94 plus -292.49 from covariance contributions) kcal/mol, free energy of the thermodynamic ensemble is -607.10 kcal/mol and frequency of the MFE structure in the ensemble is 0.00%. These differences showed the unreliability of the secondary structure of RNA in determination of function.

Seventeen (17) antibiotic compounds that have mechanism which targeted 16S rRNA was used in this study to determine their possible binding to two key enzymes that involve in 16S rRNA and tRNA activities for protein synthesis in *E. coli*. The results of molecular docking of 17 antibiotics to pseudouridine synthase RsuA (1KSV) and methyltransferase KsgA (3TPZ) in Table 2 and Figure 4, indicate that the -cycline compounds possibly have strong affinities than the -mycin compounds. The free energies from molecular docking with two enzymes used in this study, reveal possible efficacy in the following order of: doxycycline > metacycline > streptomycin > rolitetracycline > tetracycline > tigecycline. Out of 17 antibiotics in this study, chlortetracycline and minocycline have high affinity for methyltransferase KsgA, kanamycin has almost equal affinity for both enzymes while the other 14 have high affinity for pseudouridine synthase RsuA.

The results of docking simulation showed that the binding of the best 3D structure model of 16S rRNA to 1KSV and 3TPZ with free energy of -367.52 kcal/mol and-371.55 kcal/mol respectively while the ligand (protein structure) root mean square deviation (RMSD) of 262.35Å and 212.23Å for 1KSV and 3TPZ respectively (Figure 5). The active site nucleotide residues of 16S rRNA for pseudouridine synthase RsuA (1KSV) are A58, A59, C70, U71, A72, A73, A74, G75, G77, G85, U86, G87, G88, G391, C392, C393, A567, G570, A571, G572, U756, C757, G758, A759, A760, G762, C763, G980, G981, U982, C1037, A1038, G1039, U1065, G1086, A1137, C1138, U1139, C1140; and active site nucleotide residues of 16S rRNA for methyltransferase KsgA (3TPZ) are C104, G105, A114, C115, C116, U173, U174, C190, U191, U192, C201, A202, A203, U217, A218, G223, A224, C225, C226, U227, C272, G273, A274, C819, U820, A821, G854,

C868, A869, C886, G887, A888, C890, G891. Moreover, the active site nucleotide residues that may be directly interact with the active site amino acid residues of 1KSV are A59, G77, G981, U982, C1037, A1038, G1039, U1065, C1138, U1139, C1140, while that of 3TPZ are A114, C819, U820, A821, G854, G887, and A888.

The results of ligand-protein dynamics simulation of methyltransferase KsgA (3TPZ) interaction with doxycycline and methacycline (Figure 6) showed that the interaction was stable over 1 ns simulation timestep. The RMSD of atomic positions did not significantly varied with radius of gyration (Rg) in a range of 19.9 to 20.4 Å for doxycycline and 20.2 to 20.8 Å for methacycline, over the simulation time. Difference was observed in the principal component analysis (PCA) for both ligand interaction with 3TPZ, which showed conformational variation in protein structure by amino acid residues due to ligand binding. Also, the difference was evident in the molecular mechanics Poisson–Boltzmann or Generalized Born surface area (MM-PB/GBSA) of the binding. SWAXS curves that were computed from PDB structures 1KSV and 3TPZ, have Guinier fit Rg of 22.8464 Å and 20.7851 Å respectively (Figure 7). Guinier fit Rg of 3TPZ was the same as an average Rg obtained by ligand-protein MD simulation.

Table 1
Cluster of diarrhoea microbes 16 rRNA sequences **with** pintail quality obtained by search on SILVA database.

SN	Accession number	Organism
1	KX162658.1.1443; KX162656.1.1450; KY750229.1.1207; Z83205.1.1525	*Escherichia coli*
2	CP003025.16528.18064; CP003025.212088.213624; CP003025.335290.336826; CP003025.279149.280684; CP003025.271649.273185; CP003025.449268.450804	*Streptococcus lutetiensis 033*
3	CP013689.1.1531; CP013689.5810.7362; CP013689.225779.227331; CP013689.68577.70129; CP013689.284156.285708; CP013689.61083.62635; CP013689.398494.400046; CP013689.1808358.1809910; CP013689.1814190.1815742;	*Streptococcus infantarius*
4	CP007751.37529.39032; CP007751.392464.393967; CP007751.693858.695361	*Campylobacter jejuni subsp. jejuni D42a*
5	CP007749.37394.38897; CP007749.392073.393576; CP007749.684989.686492	*Campylobacter jejuni subsp. jejuni M129*
6	AF497805.1.1428	*Campylobacter upsaliensis*
7	AF326472.1.1523; AF539705.1.1503	*Enterococcus ratti*
8	AF142062.1.1430	*Helicobacter sp. 'feline isolate*
9	AF262037.1.1457	*Helicobacter canadensis*
10	AF497808.1.1475	*Anaerobiospirillum sp. B0101*
11	AF497809.1.1453	*Anaerobiospirillum sp. 3J102*
12	JQ627624.1.1441	*Prevotella; uncultured bacterium*
13	DI173490.1.1556	*Lactobacillus; unidentified*

Table 2
Binding energy score of the interaction between 16S rRNA-targeted antibiotics and two 16S rRNA enzymes, obtained from AutoDock Vina.

SN	Anti- 16S rRNA Compounds (Ligand)	DrugBank ID	Binding Free Energy (kcal/mol)	
			16S rRNA pseudouridine synthase (PDB ID: 1KSV)	16S rRNA methyltransferase KsgA (PDB ID: 3TPZ
1	Apramycin	DB04626	-11.3	-9.5
2	Chlortetracycline	DB09093	-9.9	-11.4
3	**Doxycycline**	DB00254	**-12.7**	**-12.5**
4	Gentamicin	DB00798	-9.9	-7.5
5	Kanamycin	DB01172	-9.4	-9.3
6	**Methacycline**	DB00931	**-12.7**	**-12.3**
7	Minocycline	DB01017	-9.3	-11.2
8	Neomycin	DB00994	-10.2	-9.2
9	Netilmicin	DB00955	-9.7	-8.4
10	Omadacycline	DB12455	-11.1	-9.9
11	Oxytetracycline	DB00595	**-11.7**	**-11.2**
12	Paromomycin	DB01421	-9.1	-7.0
13	Rolitetracycline	DB01301	**-12.3**	**-10.5**
14	**Streptomycin**	DB01082	**-12.6**	**-11.6**
15	Tetracycline	DB00759	**-12.2**	**-11.3**
16	Tigecycline	DB00560	**-11.9**	**-11.0**
17	Tobramycin	DB00684	-9.0	-7.3

Discussion

The pintail quality of the SILVA database checks anomalies in the sequences of SSU rRNA database on a normalized score between 0 (anomalous or chimeric) and 100 (best quality) (Pruesse et al., 2007; Ashelford et al., 2005). This study identifies microorganisms associated with diarrhea which include uncultured bacterium (*Prevotella*) and unidentified bacterium (*Lactobacillus*), whereas *E. coli*, and *C. jejuni* have been reported in another metagenomics and bioinformatics study of diarrhoea (Loman et al., 2013; Ugboko et al., 2019).

In patients with diarrhoea, gut microbiome studies have shown an increase prevalence of *Proteobacteria* and genera that contain organisms often associated with lower pH and higher oxygen levels of the upper gut, like *Lactobacillaceae* and *Enterobacteriaceae*, and a concomitant decrease in the relative abundances of Bacteroidetes and some Firmicutes (Duvallet et al., 2017; Donaldson *et al*., 2016). However, a reduction in butyrate-producing Clostridia, including genera within *Ruminococcaceae* and *Lachnospiraceae* families, have been associated with a healthy gut (Wong et al., 2006).

Ribonucleic acid is generally associated with RNA-binding proteins (RBPs) which provide serve to either protection, stabilization, processing and regulation of its activities within the cell (Hong et al., 2014). Structural similarity exists among ribosomal proteins such S6 and S4, and RsuA, which suggests evolutionary mobilization of specific domains from the 30S ribosome into the RsuA structure (Sivaraman et al., 2002). According to Burger et al. (2010), there are drugs that inhibited ribosomal RNA synthesis either at the level of (i) rRNA transcription (ii) early rRNA processing or (iii) late rRNA processing. Pseudouridine synthase is an enzyme that converts specific uridine residue to pseudouridine (5-ribosyl uracil; Ψ); an often modification in rRNA, tRNA and small nuclear RNA (snRNA) which is still remain poorly understood. Another important conserved modification in SSU of rRNAs is the dimethylation of two adjacent adenosine bases in the loop of helix 45, near the 3´-end to produce N^6, N^6-dimethyladenosine. In bacteria, this dimethylation is carried out by the enzyme identified as KsgA (O'Farrell et al., 2004). The KsgA family belongs to a well-characterized cluster of *S*-adenosyl-L-methionine (SAM)-dependent methyltransferases, known as Class I MTases, and it functionally methylated A1518 and A1519 in 16S rRNA of 30S subunit by engaging the interaction of four of its highly conserved residues in the C-terminal domain (R221, R222, K223, and R248) with helix 45 of 16S rRNA (O'Farrell et al., 2004).

In *E. coli*, pseudouridine synthase RsuA (PDB ID: 1KSV) amino acid residues interact with antibiotics in this study, which are similar to the highly conserved residues (Lys 67, Gly 99, Arg 100, Leu 101, Asp 102, Gly 107, Tyr 132, Gly 181, Arg 182, His 184, Gln 185, Leu/Ile 186, Arg 187) of the motifs found in the cluster around the deep cleft of central and C-terminal domains of pseudouridine synthase superfamily that recognizes rRNA and tRNA (Sivaraman et al., 2002). Aspartate residue D102, was proposed and confirmed to be at the reaction center of all pseudouridine synthases and responsible for production of Ψ 516 in the SSU of 16S rRNA (Koonin, 1996; Huang et al., 1998; Conrad et al., 1999).

Thus, the binding of antibiotics to this catalytic site possibly paralyses the interaction of this enzyme with RNA residue, specifically for the formation of pseudouridine. The active site amino acid residue of methyltransferase KsgA (PDB ID: 3TPZ) are Gly16, Asn113, Tyr116, Met139, Leu140-Gln141, Pro185-Lys186, and Val187. However, mutation of catalytic residues 113 and 114 in *E. coli* KsgA enzyme has no effect on its binding to the 30S subunit but resulted in similar reductions in overall enzymatic activity and this showed that the catalytic core of KsgA has direct intrinsic interaction with the RNA (O'Farrell *et al*., 2012). Thus, the result of this study claims that binding of the antibiotics to the active site of KsgA could prevent dimethylation of fully formed 30S subunit rRNA, making the active site of the enzyme inaccessible for specific of two adjacent adenosine bases.

In this study, the most represented -cycline compounds is tetracyclines. The 16S rRNA was suggested as key element in the inhibition of tRNA binding in an *in vitro* study of tetracyclines mode of action (Oehler et al., 1997), and this generally adopted mechanism, was recently challenged and call for more pragmatic evidence. Studies have indicated that base mutations in the 16S rRNA especially at positions G942 in helix 29 (h29), AGA965 or A965, G966, and A967 in h31, and G1058 in h34; confer tetracycline resistance and it pointed their involvement in tetracyclines mode of action (Chukwudi, 2016). The 16S rRNA sequence was found to be essential for ribonuclease I inhibition in *E. coli* by dysfunction or regulation of its h41 (Kitahara and Miyazaki, 2011). The evidence that tetracyclines have quite level of efficacy on RNA viruses such as human immunodeficiency virus (HIV), West Nile virus (WNV), and Japanese encephalitis virus (JEV), supported the fact that this class of drug has RNA-based mechanism of action but the actual mechanism is still poorly understood (Chukwudi, 2016).

Protein dynamics is central to all biological events such as bio-catalysis, cellular regulation and signal transduction. Ligand-driven protein dynamics contributes to an optimal understanding of protein activity (specificity and inhibition), which find application in drug discovery. Small- and wide-angle X-ray scattering (SAXS/WAXS or SWAXS) is used to probe structure of biomolecules in solution, where the density of the hydration layer is typically larger as compared to bulk solvent, and thus lead to an apparently increased radius of gyration of the solute (Knight and Hub, 2015; Merzel and Smith, 2002). Study has shown that explicit-solvent molecular dynamics (MD) simulations accurately reproduce the increase of the radius of gyration due to the hydration layer, suggesting that the simulations provide an accurate model of hydration (Chen and Hub, 2014).

Conclusion

This study provides an insight on the mechanism of action of antibiotics that targeted 16S rRNA and that proposed that the mechanism is achieved by inhibition of key enzymes involved in the protein synthesis. We have hypothesized that antibiotics bind to the 16S rRNA processing enzymes, and these enzymes in turn bind to 16S rRNA in a deactivated form which render their interaction with the active site nucleotide residues to become nonsense, and make RNA processing futile. However, in this study, microbes that causes diarrhoea was limited to those whose information meet the pintail standard of the SILVA database. The Rg obtained for free and ligand-bound methyltransferase KsgA (3TPZ) showed that actual inhibition possibly occur through subsequent binding to 16S rRNA and this revealed stepwise of interaction of these antibiotics with enzyme and rRNA. The results of this study need further validation using biophysical techniques.

Declarations

Conflict of interest

The authors have declared that there is no conflict of interest.

References

1. Ashelford KE, Chuzhanova NA, Fry JC, Jones AJ, Weightman AJ, (2005). At least 1 in 20 16S rRNA sequence records currently held in public repositories is estimated to contain substantial anomalies. *Appl. Environ. Microbiol.*, 71, 7724–7736.
2. Bernhart SH, Hofacker IL, Will S, Gruber AR, Stadler PF, (2008). RNAalifold: improved consensus structure prediction for RNA alignments. *BMC Bioinformatics*, 11;9:474
3. Burger K, Muhl B, Harasim T, Rohrmoser M, Malamoussi A, Orban M, Kellner M, Gruber-Eber A, Kremmer E, Holzel M, Dirk Eick D, (2010). Chemotherapeutic Drugs Inhibit Ribosome Biogenesis at Various Levels. *J Biol. Chem.*, 285(16): 12416–12425.
4. Chen, P. and Hub, J.S. (2014) Validating solution ensembles from molecular dynamics simulation by wide-angle X-ray scattering data. *Biophys. J.*, 107, 435–447.
5. Chukwudi CU, (2016). rRNA Binding Sites and the Molecular Mechanism of Action of the Tetracyclines. *Antimicrob. Agents Chemotherapy*, 60(8):4433–4441
6. Conrad J, Niu L, Rudd K, Lane BG, Ofengand J, (1999). 16S ribosomal RNA pseudouridine synthase RsuA of Escherichia coli: Deletion, mutation of the conserved Asp102 residue, and sequence comparison among all other pseudouridine synthases. *RNA*, 5:751–763
7. David LA, Weil A, Ryan ET, Calderwood SB, Harris JB, Chowdhury F, Begum Y, Qadri F, LaRocque RC, Turnbaugh PJ, (2015). Gut microbial succession follows acute secretory diarrhea in humans. *mBio*, 6(3):e00381-15.
8. Duvallet C, Gibbons SM, Gurry T, Irizarry RA, Alm EJ, (2017). Meta-analysis of gut microbiome studies identifies disease-specific and shared responses. *Nature Comm.*, 8: 1784.
9. Dycke JV, Arnoldi F, Papa G, Vandepoele J, Burrone OR, Mastrangelo E, Tarantino D, Heylen E, Neyts J, Rocha-Pereira J, (2018). A Single Nucleoside Viral Polymerase Inhibitor Against Norovirus, Rotavirus, and Sapovirus-Induced Diarrhea. *J. Infect. Dis.*, 20(60): 1–6.
10. Hill CJ, Lynch DB, Murphy K, Ulaszewska M, Jeffery IB, O'Shea CA, *et al.*, (2017). Evolution of gut microbiota composition from birth to 24 weeks in the INFANTMET cohort. *Microbiome*, 5:4.
11. Hong W, Zeng J, Xie J, (2014). Antibiotic drugs targeting bacterial RNAs. *Acta Pharmaceutica Sinica B*, 4(4):258–265.
12. Huang L, Pookanjanatavip M, Gu X, Santi DV, (1998). A conserved aspartate of tRNA pseudouridine synthase is essential for activity and a probable nucleophilic catalyst. *Biochemistry*, 37:344–351.
13. Huang SY, Zou X. (2014). A knowledge-based scoring function for protein-RNA interactions derived from a statistical mechanics-based iterative method. *Nucleic Acids Res.*, 42:e55.
14. Ibraheem O, Fatoki TH, Enibukun JM, Faleye BC, Momodu DM, (2019). *In Silico* Toxicological Analyses of Selected Dumpsite Contaminants on Human Health. *Nova Biotechnol. et Chimica.* 18(2):144-153
15. Kitahara K, Miyazaki K, (2011). Specific inhibition of bacterial RNase T2 by helix 41 of 16S ribosomal RNA. *Nat. Commun.* 2:549.

16. Knight CJ and Hub JS (2015). WAXSiS: a web server for the calculation of SAXS/WAXS curves based on explicit-solvent molecular dynamics. Nucleic Acids Research, 43(W1):W225-30. DOI: 10.1093/nar/gkv309
17. Koonin EV, (1996). Pseudouridine synthases: Four families of enzymes containing a putative uridine-binding motif also conserved in dUTPases and dCTP deaminases. *Nucleic Acids Res.*, 24:2411–2415.
18. Lamberti LM, Bourgeois AL, Walker CL, Black RE, Sack D. (2014). Estimating diarrhoea illness and deaths attributable to Shigellae and enterotoxigenic Escherichia coli among older children, adolescents, and adults in South Asia and Africa. *PLoS Negl. Trop. Diseases*, 8(2):e2705.
19. Letunic I, Bork P, (2019). Interactive Tree of Life (iTOL) v4: recent updates and new developments. *Nucleic Acids Res.*, 47: W256–W259.
20. Loman NJ, Constantinidou C, Christner M, Rohde H, Chan JZM, Quick J, Weir JC, Quince C, Smith GP, Betley JR, Aepfelbacher M, Pallen MJ, (2013). A Culture-Independent Sequence-Based Metagenomics Approach to the Investigation of an Outbreak of Shiga-Toxigenic *Escherichia coli* O104:H4. *JAMA*, 309(14): 1502–1510.
21. Merzel, F. and Smith, J.C. (2002) Is the first hydration shell of lysozyme of higher density than bulk water?. *Proc. Natl. Acac. Sci. U.S.A.*, 99, 5378–5383.
22. Morris GM, Huey R, Lindstrom W, Sanner M. F, Belew R. K, Goodsell D. S, *et al*. (2009). AutoDock4 and AutoDockTools4: automated docking with selective receptor flexibility. *J. Comput. Chem.*, 30(16):2785–2791.
23. O'Farrell HC, Scarsdale JN, Rife JP, (2004) Crystal structure of KsgA, a universally conserved rRNA adenine dimethyltransferase in *Escherichia coli*. *J. Mol. Biol.*, 339, 337–353.
24. Oehler R, Polacek N, Steiner G, Barta A. (1997). Interaction of tetracycline with RNA: photoincorporation into ribosomal RNA of Escherichia coli. *Nucleic Acids Res.*, 25:1219–1224.
25. O'Farrell HC, Musayev FN, Scarsdale JN, Rife JP, (2012). Control of Substrate Specificity by a Single Active Site Residue of the KsgA Methyltransferase. *Biochemistry*, 51: 466–474
26. Oldfield EC, (2002). Evaluation of Chronic Diarrhea in Patients with Human Immunodeficiency Virus Infection. *Rev Gastroenterol Disord.*, 2(4):176–188.
27. Pruesse E, Quast C, Knittel K, Fuchs BM, Ludwig W, Peplies J, Glockner FO, (2007). SILVA: a comprehensive online resource for quality checked and aligned ribosomal RNA sequence data compatible with ARB. *Nucleic Acids Res.*, 35(21):7188–7196.
28. Qin, J. *et al*. (2010). A human gut microbial gene catalogue established by metagenomic sequencing. *Nature*, 464, 59–65.
29. Quast C, Pruesse E, Yilmaz P, Gerken J, Schweer T, Yarza P, Peplies J, Glockner FO, (2013). The SILVA ribosomal RNA gene database project: improved data processing and web-based tools. *Nucleic Acids Res.*, 41: D590–D596.
30. Singh RK, Chang H-W, Yan D, Lee KM, Ucmak D, Wong K, *et al*. (2017). Influence of diet on the gut microbiome and implications for human health. *J Transl Med.*, 15:73.

31. Sivaraman, J, Sauve V, Larocque R, Stura EA, Schrag JD, Cygler M, Matte A, (2002). Structure of the 16S rRNA pseudouridine synthase RsuA bound to uracil and UMP. *Nat. Struct. Mol. Biol.*, 9: 353–358
32. Tamburini S, Shen N, Wu HC, Clemente JC, (2016). The microbiome in early life: implications for health outcomes. *Nat Med.*, 22:713–722.
33. Trott O, Olson AJ, (2010). AutoDock Vina: improving the speed and accuracy of docking with a new scoring function, efficient optimization, and multithreading. *J. Comput. Chem.*, 31(2):455–461.
34. Ugboko HU, Oranusi SU, Nwinyi OC, Fatoki TH, Akinduti PA, Enibukun JM, (2019). *In Silico* Screening and Analyses of Broad-Spectrum Molecular Targets and Lead Compounds for Diarrhoea Therapy. *Bioinformatics and Biology Insight*, 13:1-11.
35. WHO - World Health Organization (2015). Global Health Observatory Data Repository. Available from: URL: http://apps.who.int/gho/data/node.main.CODWORLD?lang=en.2015
36. Wong JMW, Souza R, Kendall CWC, Emam A, Jenkins DJA, (2006). Colonic health: fermentation and short chain fatty acids. *J. Clin. Gastroenterol*. 40, 235–243.
37. Wu H, Tremaroli V, Bäckhed F. (2015). Linking microbiota to human diseases: a systems biology perspective. *Trends Endocrinol Metab.*, 26:758–70.
38. Yan Y, Zhang D, Zhou P, Li B, Huang S-Y, (2017). HDOCK: a web server for protein-protein and protein-DNA/RNA docking based on a hybrid strategy. *Nucleic Acids Res.*, 45(W1):W365-W373.
39. Yang I, Corwin EJ, Brennan PA, Jordan S, Murphy JR, Dunlop A, (2016). The infant microbiome: implications for infant health and neurocognitive development. *Nurs Res.* 65:76–88.
40. Yang J-F, Wang F, Chen Y-Z, Hao G-Hand Yang G-F, (2019). LARMD: integration of bioinformatic resources to profile ligand-driven protein dynamics with a case on the activation of estrogen receptor. *Briefings in Bioinformatics*, 00(00), 2019, 1–13. doi: 10.1093/bib/bbz141
41. Zhang B, Bai P, Zhao X, et al. (2019). Increased growth rate and amikacin resistance of *Salmonella enteritidis* after one-month spaceflight on China's Shenzhou-11 spacecraft. *Microbiology Open*, 8:e833.

Figures

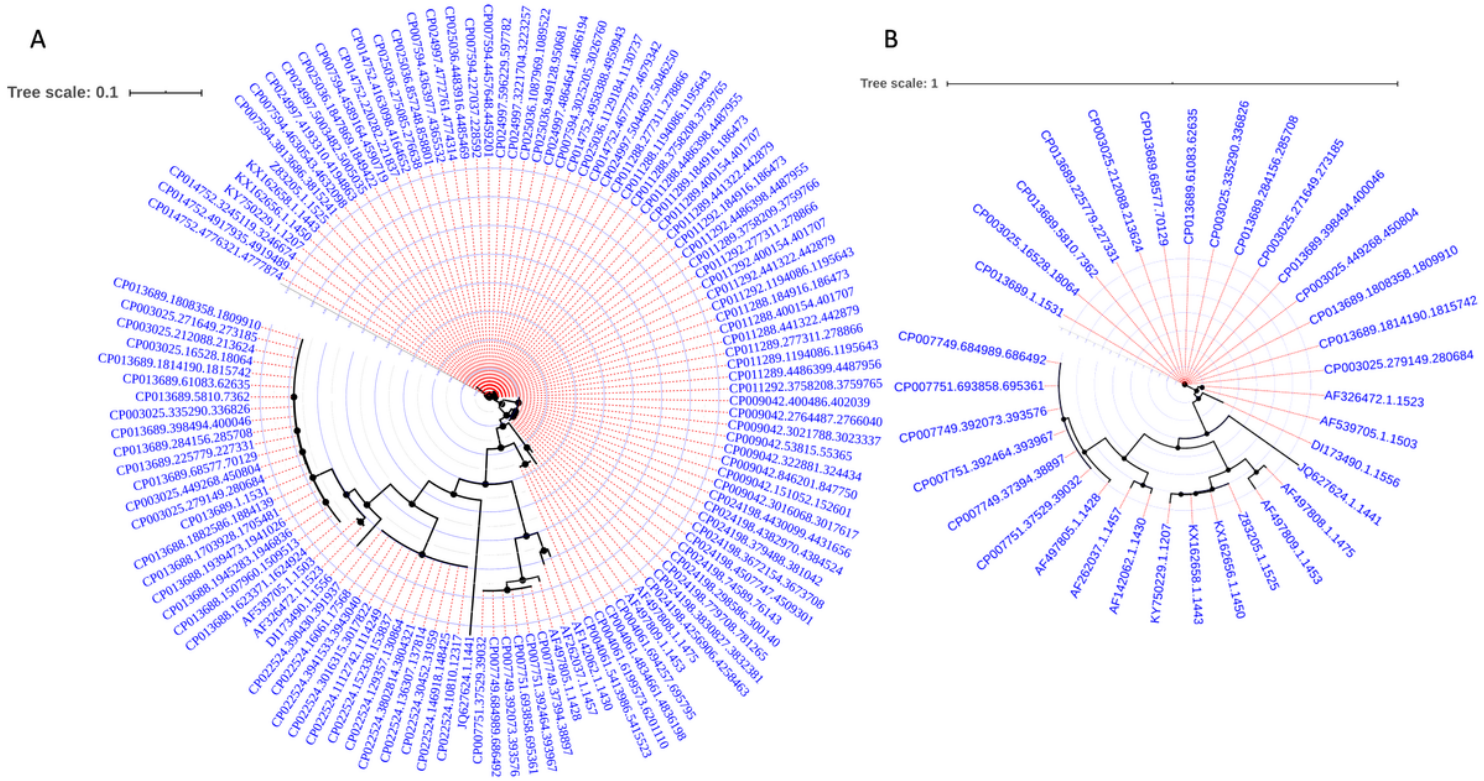

Figure 1

Phylogenetic tree from diarrhoea microbes 16 rRNA sequences (A) with and without pintail quality obtained from Aligner on SILVA database. (B) with pintail quality obtained from Aligner on SILVA database. The phylogeny was visualized at iTOL server.

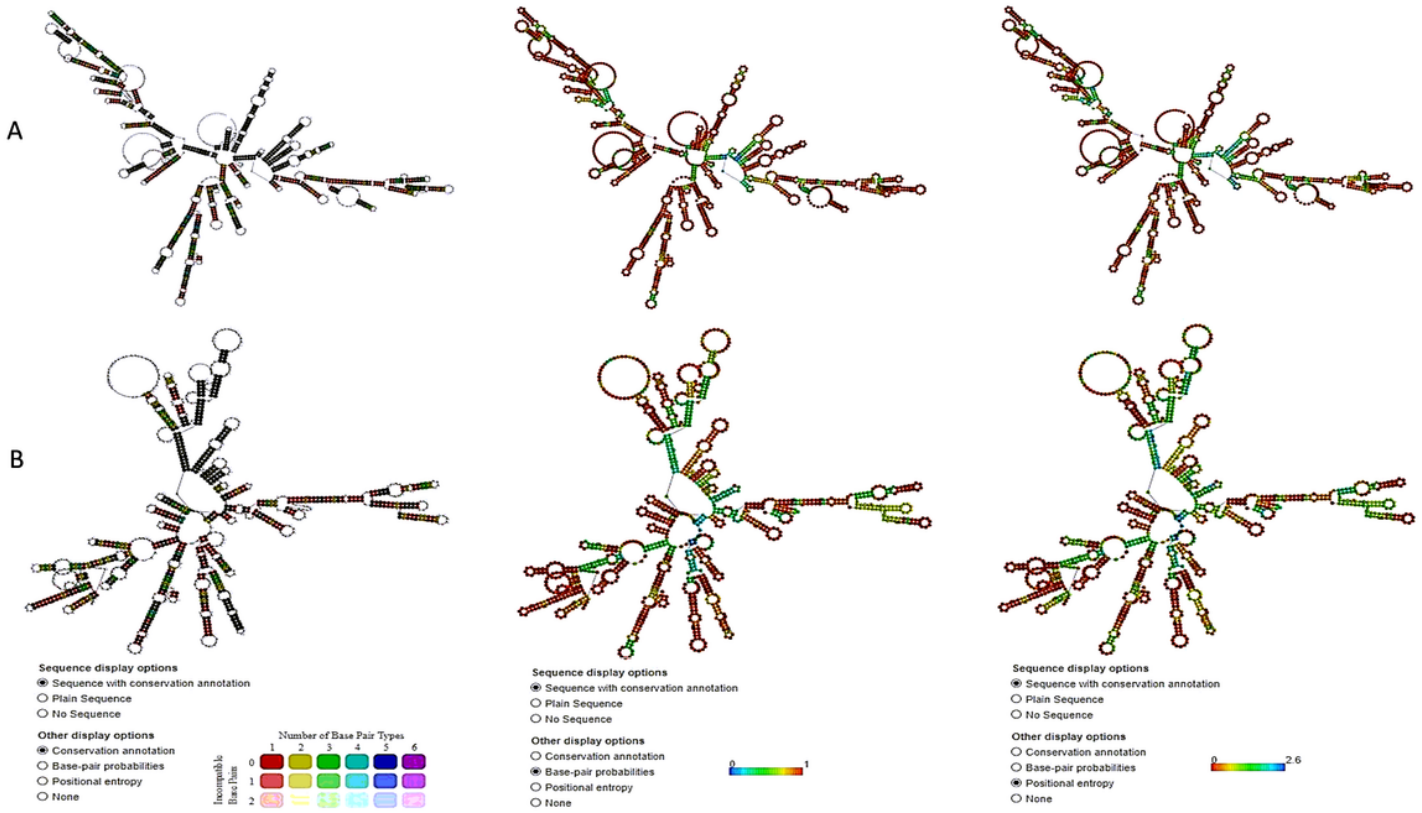

Figure 2

Consensus secondary structure of diarrhoea microbes 16 rRNA sequences with pintail quality obtained from RNAalifold server (A) queried with MSA obtained from ClustalO server. (B) queried with MSA obtained from Aligner server.

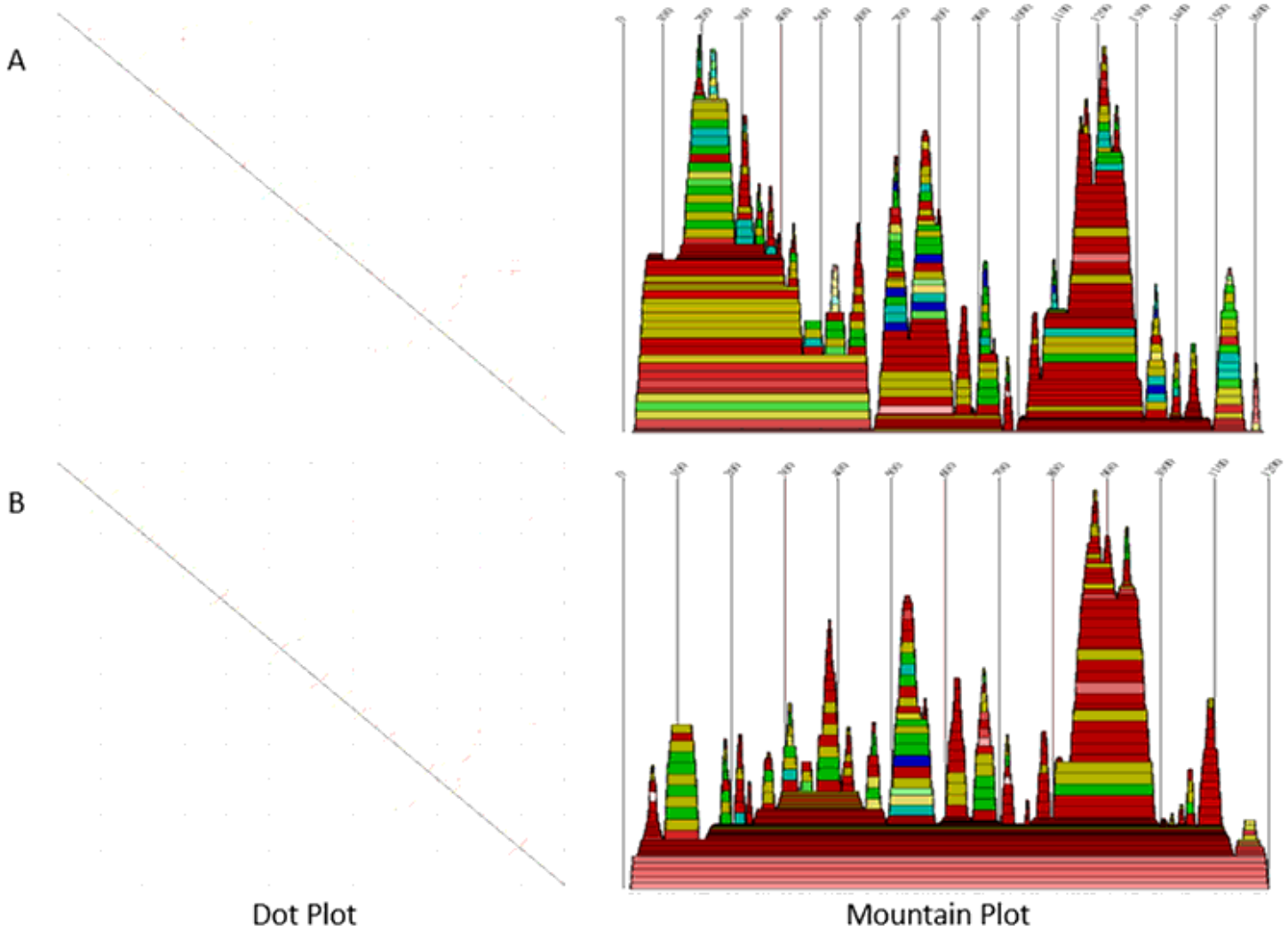

Figure 3

Dot plot and mountain plot of the consensus secondary structure of diarrhoea microbes 16 rRNA sequences with pintail quality obtained from RNAalifold server (A) queried with MSA obtained from ClustalO server. (B) queried with MSA obtained from Aligner server.

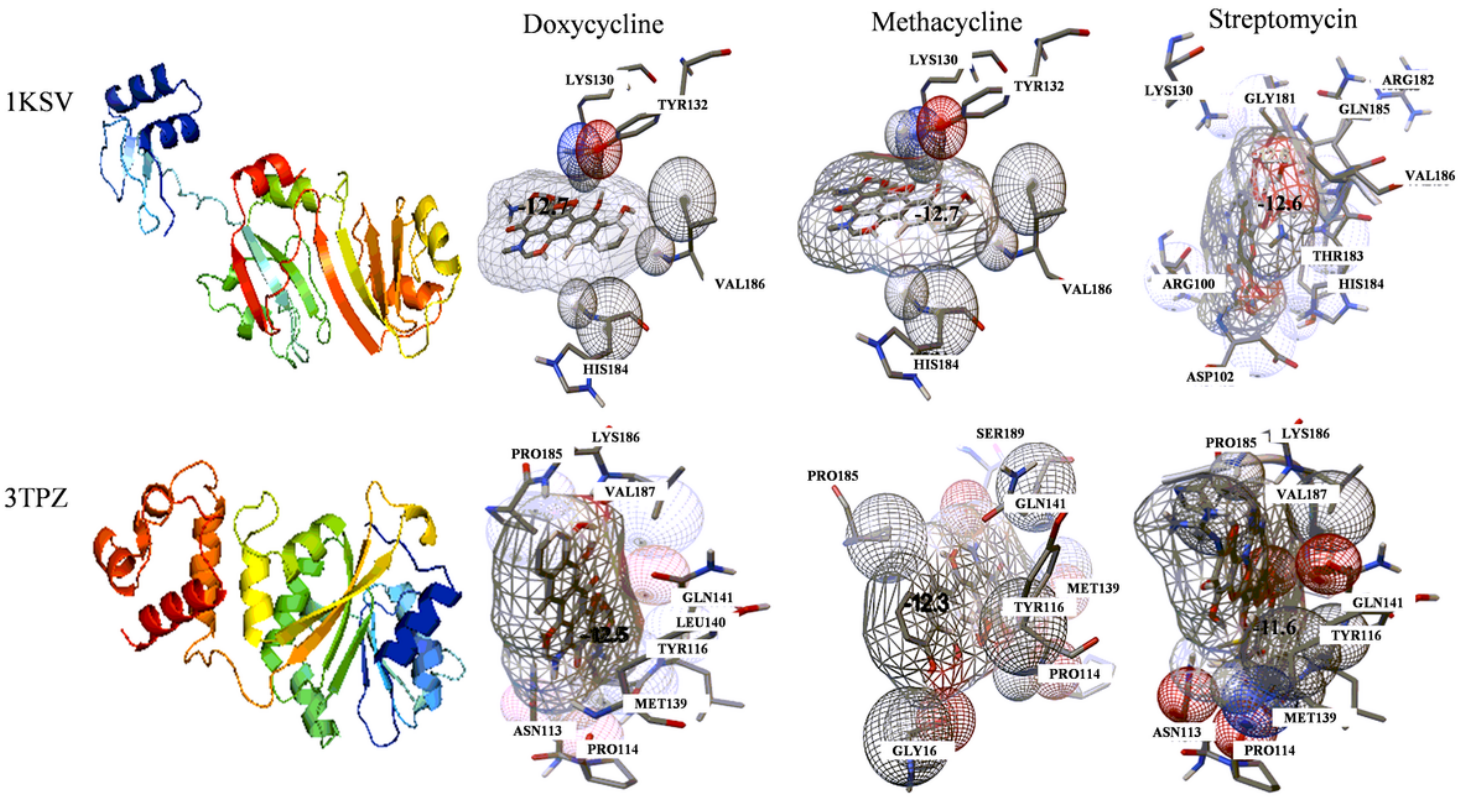

Figure 4

Binding pose of interaction of Doxycycline, Metacycline and Streptomycin with E. coli (strain K12) 16S rRNA enzymes 1KSV (pseudouridine synthase) and 3TPZ (methyltransferase KsgA), analyzed using AutoDock Vina software.

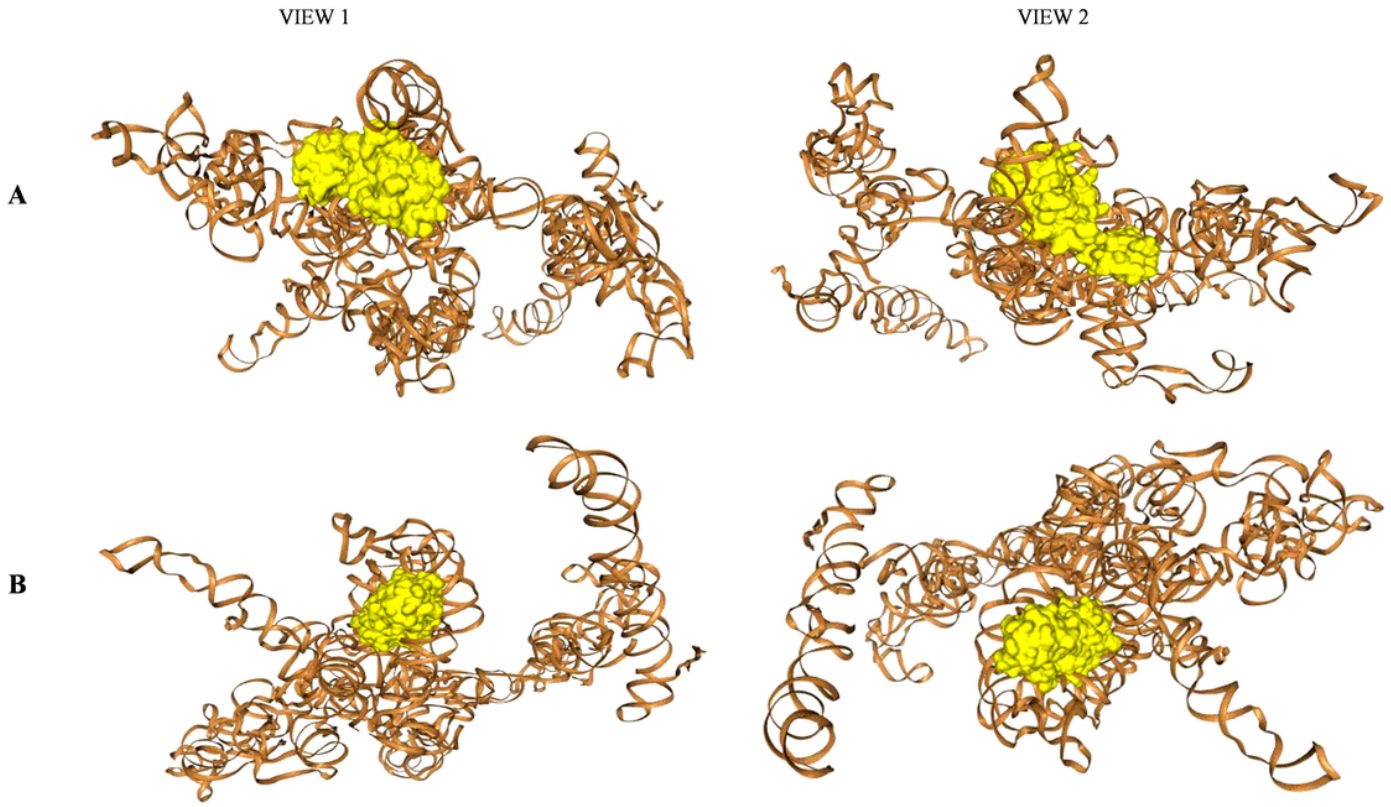

Figure 5

Binding pose of consensus 3D structure of 16S rRNA with the enzymes (area in yellow) (A) pseudouridine synthase RsuA (1KSV), (B) methyltransferase KsgA (3TPZ).

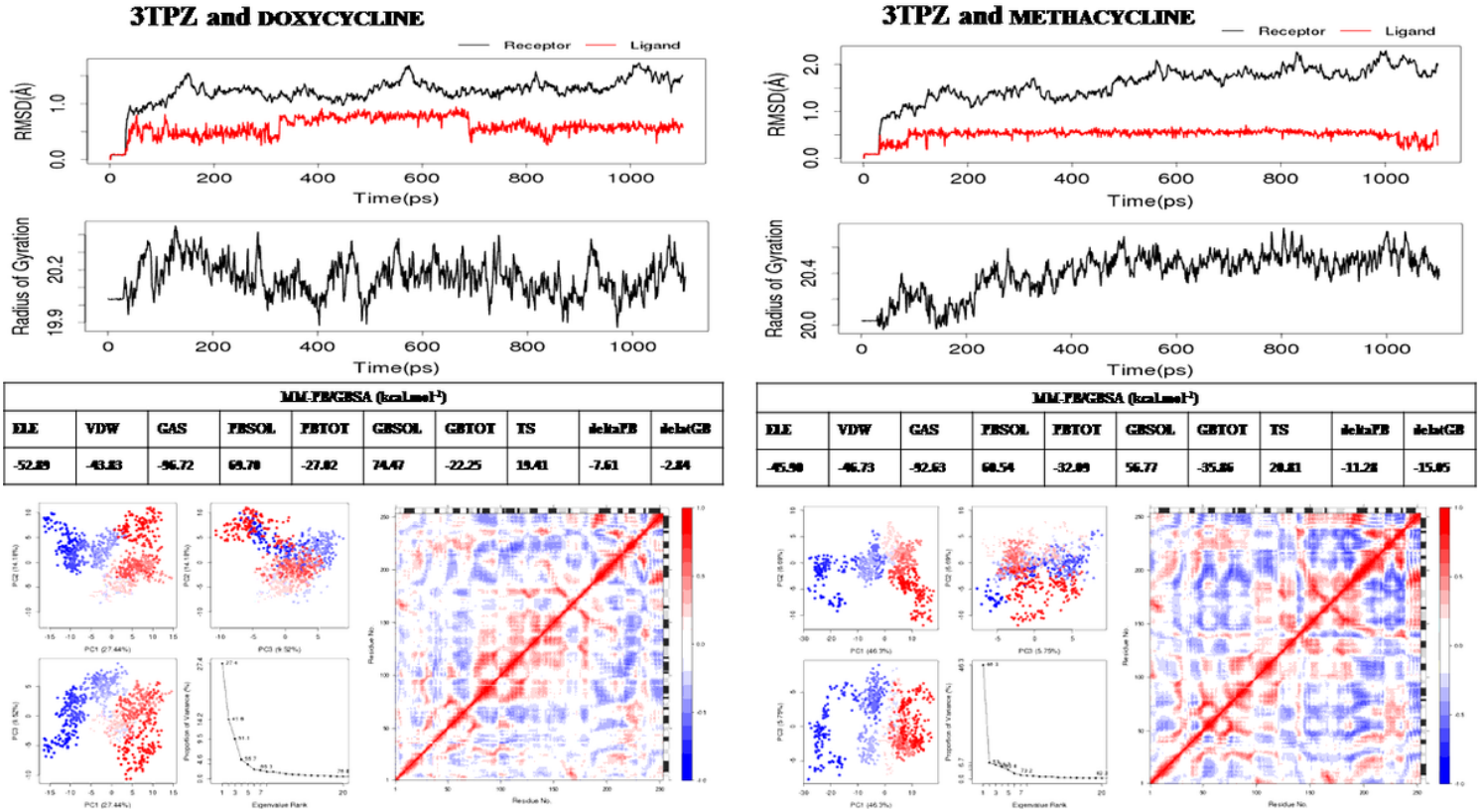

Figure 6

Ligand-Protein molecular dynamics simulation of 3TPZ interaction with Doxycycline and Methacycline. Electrostatic energy (ELE), van der Waals contribution (VDW), total gas phase energy (GAS), non-polar and polar contributions to solvation (PBSOL/GBSOL). Final estimated binding free energy (deltaPB/ deltaGB) was calculated from the terms above (PBTOT/GBTOT) and entropy (TS).

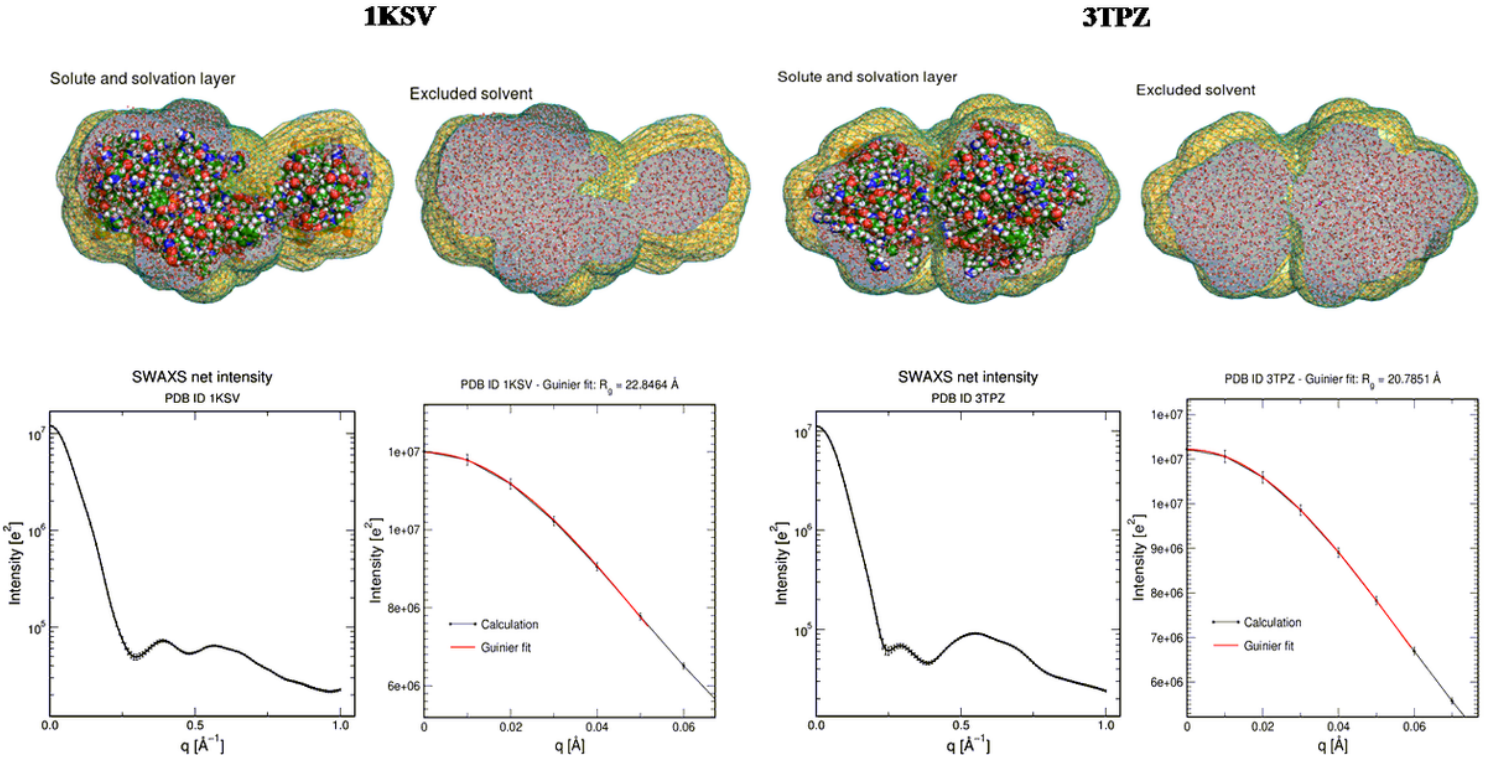

Figure 7

WAXSiS for two proteins, computed from PDB structures 1KSV and 3TPZ, showing molecular representations of solute, hydration layer and excluded solvent; SWAXS curve, as well as a Guinier fit.